

Measurement of the inclusive $B_s^0 \rightarrow X^+ \ell^- \nu$ semileptonic decay branching fraction

K. Abe,¹⁰ I. Adachi,¹⁰ H. Aihara,⁵² K. Arinstein,¹ T. Aso,⁵⁶ V. Aulchenko,¹ T. Aushev,^{22, 16}
 T. Aziz,⁴⁸ S. Bahinipati,³ A. M. Bakich,⁴⁷ V. Balagura,¹⁶ Y. Ban,³⁸ S. Banerjee,⁴⁸
 E. Barberio,²⁵ A. Bay,²² I. Bedny,¹ K. Belous,¹⁵ V. Bhardwaj,³⁷ U. Bitenc,¹⁷ S. Blyth,²⁹
 A. Bondar,¹ A. Bozek,³¹ M. Bračko,^{24, 17} J. Brodzicka,¹⁰ T. E. Browder,⁹ M.-C. Chang,⁴
 P. Chang,³⁰ Y. Chao,³⁰ A. Chen,²⁸ K.-F. Chen,³⁰ W. T. Chen,²⁸ B. G. Cheon,⁸
 C.-C. Chiang,³⁰ R. Chistov,¹⁶ I.-S. Cho,⁵⁸ S.-K. Choi,⁷ Y. Choi,⁴⁶ Y. K. Choi,⁴⁶ S. Cole,⁴⁷
 J. Dalseno,²⁵ M. Danilov,¹⁶ A. Das,⁴⁸ M. Dash,⁵⁷ J. Dragic,¹⁰ A. Drutskoy,³ S. Eidelman,¹
 D. Epifanov,¹ S. Fratina,¹⁷ H. Fujii,¹⁰ M. Fujikawa,²⁷ N. Gabyshev,¹ A. Garmash,⁴⁰
 A. Go,²⁸ G. Gokhroo,⁴⁸ P. Goldenzweig,³ B. Golob,^{23, 17} M. Grosse Perdekamp,^{12, 41}
 H. Guler,⁹ H. Ha,¹⁹ J. Haba,¹⁰ K. Hara,²⁶ T. Hara,³⁶ Y. Hasegawa,⁴⁵ N. C. Hastings,⁵²
 K. Hayasaka,²⁶ H. Hayashii,²⁷ M. Hazumi,¹⁰ D. Heffernan,³⁶ T. Higuchi,¹⁰ L. Hinz,²²
 H. Hoedlmoser,⁹ T. Hokuue,²⁶ Y. Horii,⁵¹ Y. Hoshi,⁵⁰ K. Hoshina,⁵⁵ S. Hou,²⁸
 W.-S. Hou,³⁰ Y. B. Hsiung,³⁰ H. J. Hyun,²¹ Y. Igarashi,¹⁰ T. Iijima,²⁶ K. Ikado,²⁶
 K. Inami,²⁶ A. Ishikawa,⁴² H. Ishino,⁵³ R. Itoh,¹⁰ M. Iwabuchi,⁶ M. Iwasaki,⁵² Y. Iwasaki,¹⁰
 C. Jacoby,²² N. J. Joshi,⁴⁸ M. Kaga,²⁶ D. H. Kah,²¹ H. Kaji,²⁶ S. Kajiwara,³⁶
 H. Kakuno,⁵² J. H. Kang,⁵⁸ P. Kapusta,³¹ S. U. Kataoka,²⁷ N. Katayama,¹⁰ H. Kawai,²
 T. Kawasaki,³³ A. Kibayashi,¹⁰ H. Kichimi,¹⁰ H. J. Kim,²¹ H. O. Kim,⁴⁶ J. H. Kim,⁴⁶
 S. K. Kim,⁴⁴ Y. J. Kim,⁶ K. Kinoshita,³ S. Korpar,^{24, 17} Y. Kozakai,²⁶ P. Križan,^{23, 17}
 P. Krokovny,¹⁰ R. Kumar,³⁷ E. Kurihara,² A. Kusaka,⁵² A. Kuzmin,¹ Y.-J. Kwon,⁵⁸
 J. S. Lange,⁵ G. Leder,¹⁴ J. Lee,⁴⁴ J. S. Lee,⁴⁶ M. J. Lee,⁴⁴ S. E. Lee,⁴⁴ T. Lesiak,³¹
 J. Li,⁹ A. Limosani,²⁵ S.-W. Lin,³⁰ Y. Liu,⁶ D. Liventsev,¹⁶ J. MacNaughton,¹⁰
 G. Majumder,⁴⁸ F. Mandl,¹⁴ D. Marlow,⁴⁰ T. Matsumura,²⁶ A. Matyja,³¹ S. McOnie,⁴⁷
 T. Medvedeva,¹⁶ Y. Mikami,⁵¹ W. Mitaroff,¹⁴ K. Miyabayashi,²⁷ H. Miyake,³⁶ H. Miyata,³³
 Y. Miyazaki,²⁶ R. Mizuk,¹⁶ G. R. Moloney,²⁵ T. Mori,²⁶ J. Mueller,³⁹ A. Murakami,⁴²
 T. Nagamine,⁵¹ Y. Nagasaka,¹¹ Y. Nakahama,⁵² I. Nakamura,¹⁰ E. Nakano,³⁵ M. Nakao,¹⁰
 H. Nakayama,⁵² H. Nakazawa,²⁸ Z. Natkaniec,³¹ K. Neichi,⁵⁰ S. Nishida,¹⁰ K. Nishimura,⁹
 Y. Nishio,²⁶ I. Nishizawa,⁵⁴ O. Nitoh,⁵⁵ S. Noguchi,²⁷ T. Nozaki,¹⁰ A. Ogawa,⁴¹
 S. Ogawa,⁴⁹ T. Ohshima,²⁶ S. Okuno,¹⁸ S. L. Olsen,⁹ S. Ono,⁵³ W. Ostrowicz,³¹
 H. Ozaki,¹⁰ P. Pakhlov,¹⁶ G. Pakhlova,¹⁶ H. Palka,³¹ C. W. Park,⁴⁶ H. Park,²¹
 K. S. Park,⁴⁶ N. Parslow,⁴⁷ L. S. Peak,⁴⁷ M. Pernicka,¹⁴ R. Pestotnik,¹⁷ M. Peters,⁹
 L. E. Piilonen,⁵⁷ A. Poluektov,¹ J. Rorie,⁹ M. Rozanska,³¹ H. Sahoo,⁹ Y. Sakai,¹⁰
 H. Sakaue,³⁵ N. Sasao,²⁰ T. R. Sarangi,⁶ N. Satoyama,⁴⁵ K. Sayeed,³ T. Schietinger,²²
 O. Schneider,²² P. Schönmeier,⁵¹ J. Schümann,¹⁰ C. Schwanda,¹⁴ A. J. Schwartz,³
 R. Seidl,^{12, 41} A. Sekiya,²⁷ K. Senyo,²⁶ M. E. Sevier,²⁵ L. Shang,¹³ M. Shapkin,¹⁵
 C. P. Shen,¹³ H. Shibuya,⁴⁹ S. Shinomiya,³⁶ J.-G. Shiu,³⁰ B. Shwartz,¹ J. B. Singh,³⁷
 A. Sokolov,¹⁵ E. Solovieva,¹⁶ A. Somov,³ S. Stanić,³⁴ M. Starič,¹⁷ J. Stypula,³¹
 A. Sugiyama,⁴² K. Sumisawa,¹⁰ T. Sumiyoshi,⁵⁴ S. Suzuki,⁴² S. Y. Suzuki,¹⁰ O. Tajima,¹⁰
 F. Takasaki,¹⁰ K. Tamai,¹⁰ N. Tamura,³³ M. Tanaka,¹⁰ N. Taniguchi,²⁰ G. N. Taylor,²⁵
 Y. Teramoto,³⁵ I. Tikhomirov,¹⁶ K. Trabelsi,¹⁰ Y. F. Tse,²⁵ T. Tsuboyama,¹⁰ K. Uchida,⁹

Y. Uchida,⁶ S. Uehara,¹⁰ K. Ueno,³⁰ T. Uglov,¹⁶ Y. Unno,⁸ S. Uno,¹⁰ P. Urquijo,²⁵
Y. Ushiroda,¹⁰ Y. Usov,¹ G. Varner,⁹ K. E. Varvell,⁴⁷ K. Vervink,²² S. Villa,²²
A. Vinokurova,¹ C. C. Wang,³⁰ C. H. Wang,²⁹ J. Wang,³⁸ M.-Z. Wang,³⁰ P. Wang,¹³
X. L. Wang,¹³ M. Watanabe,³³ Y. Watanabe,¹⁸ R. Wedd,²⁵ J. Wicht,²² L. Widhalm,¹⁴
J. Wiechczynski,³¹ E. Won,¹⁹ B. D. Yabsley,⁴⁷ A. Yamaguchi,⁵¹ H. Yamamoto,⁵¹
M. Yamaoka,²⁶ Y. Yamashita,³² M. Yamauchi,¹⁰ C. Z. Yuan,¹³ Y. Yusa,⁵⁷ C. C. Zhang,¹³
L. M. Zhang,⁴³ Z. P. Zhang,⁴³ V. Zhilich,¹ V. Zhulanov,¹ A. Zupanc,¹⁷ and N. Zwahlen²²

(Belle Collaboration)

¹*Budker Institute of Nuclear Physics, Novosibirsk*

²*Chiba University, Chiba*

³*University of Cincinnati, Cincinnati, Ohio 45221*

⁴*Department of Physics, Fu Jen Catholic University, Taipei*

⁵*Justus-Liebig-Universität Gießen, Gießen*

⁶*The Graduate University for Advanced Studies, Hayama*

⁷*Gyeongsang National University, Chinju*

⁸*Hanyang University, Seoul*

⁹*University of Hawaii, Honolulu, Hawaii 96822*

¹⁰*High Energy Accelerator Research Organization (KEK), Tsukuba*

¹¹*Hiroshima Institute of Technology, Hiroshima*

¹²*University of Illinois at Urbana-Champaign, Urbana, Illinois 61801*

¹³*Institute of High Energy Physics,*

Chinese Academy of Sciences, Beijing

¹⁴*Institute of High Energy Physics, Vienna*

¹⁵*Institute of High Energy Physics, Protvino*

¹⁶*Institute for Theoretical and Experimental Physics, Moscow*

¹⁷*J. Stefan Institute, Ljubljana*

¹⁸*Kanagawa University, Yokohama*

¹⁹*Korea University, Seoul*

²⁰*Kyoto University, Kyoto*

²¹*Kyungpook National University, Taegu*

²²*École Polytechnique Fédérale de Lausanne (EPFL), Lausanne*

²³*University of Ljubljana, Ljubljana*

²⁴*University of Maribor, Maribor*

²⁵*University of Melbourne, School of Physics, Victoria 3010*

²⁶*Nagoya University, Nagoya*

²⁷*Nara Women's University, Nara*

²⁸*National Central University, Chung-li*

²⁹*National United University, Miao Li*

³⁰*Department of Physics, National Taiwan University, Taipei*

³¹*H. Niewodniczanski Institute of Nuclear Physics, Krakow*

³²*Nippon Dental University, Niigata*

³³*Niigata University, Niigata*

³⁴*University of Nova Gorica, Nova Gorica*

³⁵*Osaka City University, Osaka*

³⁶*Osaka University, Osaka*

³⁷*Panjab University, Chandigarh*

- ³⁸*Peking University, Beijing*
³⁹*University of Pittsburgh, Pittsburgh, Pennsylvania 15260*
⁴⁰*Princeton University, Princeton, New Jersey 08544*
⁴¹*RIKEN BNL Research Center, Upton, New York 11973*
⁴²*Saga University, Saga*
⁴³*University of Science and Technology of China, Hefei*
⁴⁴*Seoul National University, Seoul*
⁴⁵*Shinshu University, Nagano*
⁴⁶*Sungkyunkwan University, Suwon*
⁴⁷*University of Sydney, Sydney, New South Wales*
⁴⁸*Tata Institute of Fundamental Research, Mumbai*
⁴⁹*Toho University, Funabashi*
⁵⁰*Tohoku Gakuin University, Tagajo*
⁵¹*Tohoku University, Sendai*
⁵²*Department of Physics, University of Tokyo, Tokyo*
⁵³*Tokyo Institute of Technology, Tokyo*
⁵⁴*Tokyo Metropolitan University, Tokyo*
⁵⁵*Tokyo University of Agriculture and Technology, Tokyo*
⁵⁶*Toyama National College of Maritime Technology, Toyama*
⁵⁷*Virginia Polytechnic Institute and State University, Blacksburg, Virginia 24061*
⁵⁸*Yonsei University, Seoul*

Abstract

Inclusive semileptonic $B_s^0 \rightarrow X^+\ell^-\nu$ decays are studied for the first time using a 23.6 fb^{-1} data sample collected on the $\Upsilon(5S)$ resonance with the Belle detector at the KEKB asymmetric energy e^+e^- collider. These decays are identified by the means of a lepton accompanied by a same-sign D_s^+ meson originating from the other B_s^0 in the event. The semileptonic branching fractions are measured in the electron and muon channels to be $\mathcal{B}(B_s^0 \rightarrow X^+e^-\nu) = (10.9 \pm 1.0 \pm 0.9)\%$ and $\mathcal{B}(B_s^0 \rightarrow X^+\mu^-\nu) = (9.2 \pm 1.0 \pm 0.8)\%$, respectively. Assuming an equal electron and muon production rate in B_s^0 decays, a combined fit yields an average leptonic branching fraction $\mathcal{B}(B_s^0 \rightarrow X^+\ell^-\nu) = (10.2 \pm 0.8 \pm 0.9)\%$.

PACS numbers: 13.25.Gv, 13.25.Hw, 14.40.Gx, 14.40.Nd

Although B_s^0 mesons have been studied by LEP and Tevatron experiments for a long time, only a few B_s^0 decay branching fractions have been measured [1]. In addition to these very high energy experiments, an alternative source of B_s^0 mesons has been explored recently, where B_s^0 mesons are produced by e^+e^- colliders running at the $\Upsilon(5S)$ energy. First evidence for inclusive and exclusive B_s^0 decays at the $\Upsilon(5S)$ was found by the CLEO collaboration [2, 3], which collected a data sample of 0.42 fb^{-1} , and by the Belle collaboration [4, 5], which used a data sample of 1.86 fb^{-1} . However, the statistical significance of these first measurements was very limited. In 2006 the Belle collaboration collected an additional 21.7 fb^{-1} of data at the $\Upsilon(5S)$, allowing one to study several B_s^0 decay modes with improved statistical accuracy.

One of the most interesting B_s^0 decay modes, for which the branching fraction can be measured for the first time using the new $\Upsilon(5S)$ data, is the total inclusive semileptonic decay $B_s^0 \rightarrow X^+ \ell^- \nu$. Charge-conjugate modes are implicitly implied everywhere in this paper. The e^+e^- collisions at the $\Upsilon(5S)$ resonance are well-suited for the $\mathcal{B}(B_s^0 \rightarrow X^+ \ell^- \nu)$ measurement, while it is probably unfeasible at very high energy colliders.

Historically, the total inclusive semileptonic $B^{(0/+)} \rightarrow X \ell \nu$ decay branching fraction was measured many years ago using data obtained at the $\Upsilon(4S)$ (see PDG for the full list of the measurements [1]). The measured values covered the range of 9.7 to 11.0% (the most recent PDG average value is $(10.78 \pm 0.18)\%$) and were in a poor agreement with the theoretically predicted branching fraction of about 12% [6]. Later, explanations for this difference were proposed in several theoretical papers [7–10]; however this discrepancy is not yet completely understood.

Measurements of the total semileptonic B^0 , B^+ and B_s^0 branching fractions, together with corresponding well-measured lifetimes, determine the semileptonic widths. These widths for the B^0 , B^+ and B_s^0 mesons are expected to be equal, neglecting small corrections due to electromagnetic and light quark mass difference effects. If any significant difference between the B^0 , B^+ and B_s^0 semileptonic widths were observed, it would indicate an unknown source of lepton production in B decays.

The correlated production of a D_s^+ meson and a same-sign lepton at the $\Upsilon(5S)$ resonance is used in this analysis to measure $\mathcal{B}(B_s^0 \rightarrow X^+ \ell^- \nu)$. The method exploits the fact that, at the $\Upsilon(5S)$, the dominant production of a D_s^+ meson and a same-sign fast lepton comes from the $B_s^{(*)} \bar{B}_s^{(*)}$ state. Neither the $c\bar{c}$ continuum nor $B^{(*)} \bar{B}^{(*)}$ states (except for a small contribution due to $\sim 19\%$ B^0 mixing effect) can result in a same-sign c -quark (i.e., D_s^+ meson) and primary lepton final state. Simultaneous production of a same-sign D_s^+ meson and ℓ^+ from one B_s^0 decay is totally negligible.

BELLE DETECTOR AND DATA SAMPLES

The data were collected with the Belle detector at KEKB [11], an asymmetric energy double storage ring collider with $\sim 8.2 \text{ GeV}$ electrons and $\sim 3.6 \text{ GeV}$ positrons. In this analysis, a data sample of 23.6 fb^{-1} taken at the $\Upsilon(5S)$ CM energy of $\sim 10869 \text{ MeV}$ is used. A data sample of 40.0 fb^{-1} taken in the continuum, 60 MeV in center-of-mass energy below the $\Upsilon(4S)$, and a data sample of 64.9 fb^{-1} taken at the $\Upsilon(4S)$ resonance energy, were also used for this analysis. The continuum and $\Upsilon(4S)$ data, which were collected with the same vertex detector, provide comparable detector systematics. All experimental conditions of data-taking at the $\Upsilon(5S)$ were nearly the same as at the $\Upsilon(4S)$ or continuum runs except for beam energies and luminosities.

The Belle detector is a general-purpose large-solid-angle magnetic spectrometer that consists of a silicon vertex detector (SVD), a central drift chamber (CDC), an array of aerogel threshold Cherenkov counters (ACC), a barrel-like arrangement of time-of-flight scintillation counters (TOF), and an electromagnetic calorimeter comprised of CsI(Tl) crystals (ECL) located inside a superconducting solenoidal coil with a 1.5 T magnetic field. An iron flux-return located outside the coil is instrumented to detect K_L^0 mesons and to identify muons (KLM). The detector is described in detail elsewhere [12]. A GEANT-based detailed simulation of the Belle detector is used to produce Monte Carlo (MC) event samples and determine efficiencies.

SELECTIONS

Charged tracks are reconstructed using hit information from the CDC and SVD. Kaon and pion mass hypotheses are assigned to the charged tracks using a likelihood ratio $\mathcal{L}_{K/\pi} = \mathcal{L}_K/(\mathcal{L}_K + \mathcal{L}_\pi)$; the likelihood \mathcal{L} is obtained by combining information from the CDC (specific ionization (dE/dx)), TOF, and ACC. We require $\mathcal{L}_{K/\pi} > 0.6$ ($\mathcal{L}_{K/\pi} < 0.6$) for kaon (pion) candidates [12]. The resulting identification efficiency varies from 86% to 91% (94% to 98%) for kaons (pions), depending on the momentum.

Standard procedures are used to identify leptons. Electrons are identified using a combination of the specific ionization measurement from the CDC, the ACC response, and the electromagnetic shower position, shape and energy measurements from the ECL [13]. The electron identification probability is required to exceed 0.5. Muons are identified with KLM hit positions and penetration depth [14]; the standard muon prerejection cuts are applied and the muon likelihood ratio is required to be larger than 0.8. With these requirements, the combined reconstruction and identification efficiency is flat in momentum and around (75–78)% for both electrons and muons with momentum larger than 1 GeV/c. The efficiency decreases with momentum in the lower momentum region. Lepton tracks are required to satisfy $dr < 2$ cm and $|dz| < 5$ cm, where dr and $|dz|$ are the distances of closest approach to the nominal interaction point in the plane perpendicular to the beam axis (r – ϕ plane) and along the beam direction, respectively. To remove leptons produced in J/ψ decays and photon conversions, we require $|M(J/\psi) - M(e^+h^-)| > 50$ MeV/c², $|M(J/\psi) - M(\mu^+h^-)| > 50$ MeV/c² and $M(e^+e^-) > 100$ MeV/c², where h^- is any charged particle and $e^+(\mu^+)$ is any identified electron (muon) reconstructed in the event. Charge-conjugate combinations are also implied. Finally, momentum requirements $P(e^+) > 0.5$ GeV/c and $P(\mu^+) > 0.8$ GeV/c in the center-of-mass (CM) system are applied, and the polar angle requirements $17^\circ < \theta(e^+) < 150^\circ$ and $25^\circ < \theta(\mu^+) < 145^\circ$ in the laboratory system are applied to select regions of high reconstruction efficiency.

Only the cleanest decay mode $D_s^+ \rightarrow \phi\pi^+$ is used to measure the D_s^+ meson yield. The invariant mass of $\phi \rightarrow K^+K^-$ candidates is required to be within ± 12 MeV/c² of the nominal ϕ mass. The ϕ helicity angle distribution is expected to be proportional to $\cos^2\theta_{\text{hel}}^\phi$; therefore, the requirement $|\cos\theta_{\text{hel}}^\phi| > 0.25$ is applied. The helicity angle θ_{hel}^ϕ is defined as the angle between the directions of the K^+ and D_s^+ momenta in the ϕ rest frame. Although the D_s^+ mass resolution in the kinematic region studied is only (4–5) MeV/c², we select $\phi\pi^+$ combinations within ± 50 MeV/c² of the nominal D_s^+ mass, because sufficient sidebands are needed to fit the D_s^+ signal.

The large background under the D_s^+ signal from $e^+e^- \rightarrow q\bar{q}$ continuum events ($q = u, d, s$, or c) is significantly suppressed by the D_s^+ selection requirements and, additionally, by

the same-sign lepton requirement. Therefore, to avoid uncertainties due to a variation of selection efficiency between the $\Upsilon(5S)$, $\Upsilon(4S)$ and continuum data samples, no topological cuts are applied in this analysis to suppress continuum.

The B_s^0 mesons are produced at the $\Upsilon(5S)$ through the intermediate $B_s\bar{B}_s$, $B_s^*\bar{B}_s$, $B_s\bar{B}_s^*$ or $B_s^*\bar{B}_s^*$ channels, with subsequent $B_s^* \rightarrow B_s\gamma$ decay. These channels are not separated in this analysis; the signal MC simulation generates 93% of events in the $B_s^*\bar{B}_s^*$ channel, and 7% of events in the $B_s^*\bar{B}_s$ and $B_s\bar{B}_s^*$ channels. The $b\bar{b}$ production cross-section at the $\Upsilon(5S)$ has been measured in Ref. [4] to be $\sigma_{b\bar{b}}^{\Upsilon(5S)} = 0.302 \pm 0.015$ nb, and the fraction of $B_s^{(*)}\bar{B}_s^{(*)}$ events over all $b\bar{b}$ events is taken from the PDG [1]: $f_s = (19.5_{-2.2}^{+3.0})\%$.

NUMBER OF D_s^+ MESONS FROM B_s^0 DECAYS

To obtain the number of D_s^+ mesons produced from B_s^0 decays, we compare the normalized D_s^+ momentum distribution in the $\Upsilon(5S)$, $\Upsilon(4S)$ and continuum data samples using a procedure similar to that described in Ref.[4]. The normalized momentum is defined as $x(D_s^+) = P(D_s^+)/P_{\max}(D_s^+)$, where $P(D_s^+)$ is the D_s^+ momentum in the CM, and $P_{\max}(D_s^+)$ is the expected D_s^+ momentum if the D_s^+ were produced in the process $e^+e^- \rightarrow D_s^+D_s^-$ at the same CM energy.

The comparison of the normalized momentum $x(D_s^+)$ distributions of the $\Upsilon(5S)$ and continuum data samples (Fig. 1a) and of the $\Upsilon(4S)$ and continuum data samples (Fig. 1b) shows excellent agreement in the region $x(D_s^+) > 0.5$, where $b\bar{b}$ events cannot contribute. The continuum distributions are normalized using the energy-corrected luminosity ratio. To obtain these distributions, the D_s^+ mass spectra are fitted by a Gaussian to describe the signal and a linear function to describe the background in each bin of $x(D_s^+)$. The Gaussian width is fixed to the value obtained from MC simulation; the Gaussian mean is fixed to that obtained from fitting the D_s^+ signal in the whole $x(D_s^+) < 0.5$ range. The signal normalization and the background parameters are allowed to float.

Continuum contributions were subtracted from the $x(D_s)$ distributions for the $\Upsilon(5S)$ and $\Upsilon(4S)$ data samples (Fig. 1), and the obtained distributions are used to calculate the number of D_s^+ mesons produced from B_s^0 decays. The $\Upsilon(4S)$ distribution is normalized to the number of the $b\bar{b}$ pairs produced at the $\Upsilon(5S)$ that do not hadronize to B_s^0 mesons. To obtain this normalization, we use the number of $B\bar{B}$ pairs in our $\Upsilon(4S)$ sample, $N^{\Upsilon(4S)}(B\bar{B}) = (70.95 \pm 0.79) \times 10^6$. The number of $b\bar{b}$ pairs in the $\Upsilon(5S)$ data sample that do not hadronize to B_s^0 mesons is obtained from the formula:

$$N_{b\bar{b}}^{\Upsilon(5S)}(B\bar{B}) = \mathcal{L}_{\Upsilon(5S)} \times \sigma_{b\bar{b}}^{\Upsilon(5S)} \times (1 - f_s) \quad (1)$$

Finally, this normalization is calculated, $N_{b\bar{b}}^{\Upsilon(5S)}(B\bar{B})/N^{\Upsilon(4S)}(B\bar{B}) = 1/(12.37 \pm 0.79)$. We find that about 2/3 of D_s^+ mesons produced at the $\Upsilon(5S)$ originate from B_s^0 decays. After the $B\bar{B}$ contribution is subtracted and all bins are summed over the interval $x(D_s) < 0.5$, the number of D_s^+ mesons produced from B_s^0 decays is obtained: $N(B_s^0 \rightarrow D_s^+ X) = 13434 \pm 357(stat) \pm 479(syst)$.

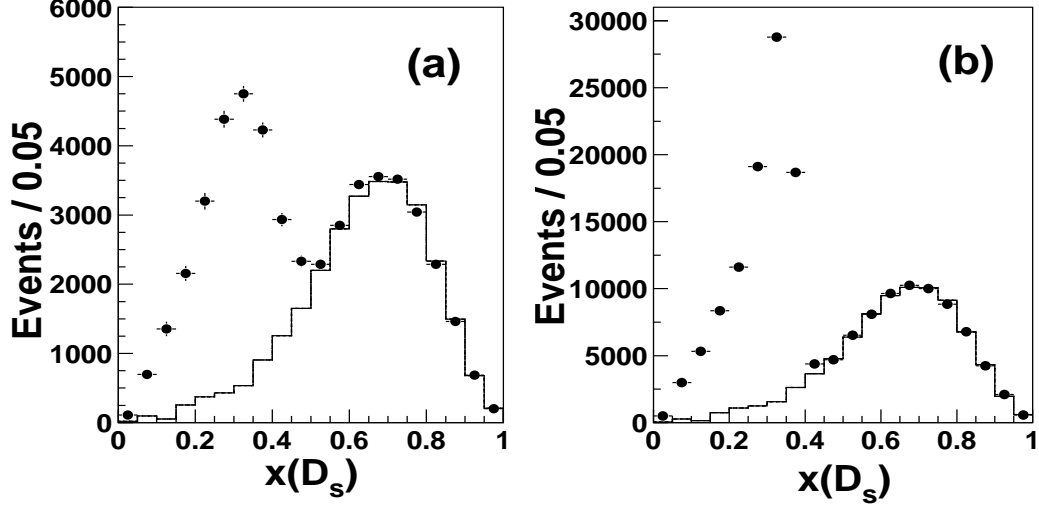


FIG. 1: Comparison of the D_s^+ normalized momenta $x(D_s^+)$ for the $\Upsilon(5S)$ and continuum data samples (a), and for the $\Upsilon(4S)$ and continuum data samples (b). The points with error bars are the $\Upsilon(5S)$ and $\Upsilon(4S)$ data, while the histograms show the normalized continuum.

SAME-SIGN D_s^+ AND LEPTON EVENTS IN $\Upsilon(5S)$ SAMPLE

The number of same-sign D_s^+ and lepton events is obtained at the $\Upsilon(5S)$, $\Upsilon(4S)$ and continuum data samples as a function of lepton momentum for the whole D_s^+ momentum range $0 < P(D_s^+) < 2.6 \text{ GeV}/c$. To obtain these distributions, the D_s^+ mass spectra are fitted in each bin of $P(\ell^-)$ in a manner similar to that described in the previous section.

The following backgrounds must be subtracted from the $\Upsilon(5S)$ data to obtain the same-sign D_s^+ and lepton events from B_s^0 decays:

- 1 Background due to $\Upsilon(5S) \rightarrow B\bar{B}(X)$ decays. This is the dominant background, which is evaluated using the momentum-corrected $\Upsilon(4S) \rightarrow B\bar{B}$ data.
- 2 Background due to continuum under the $\Upsilon(5S)$ resonance. This background is significantly suppressed by the lepton requirement. It is evaluated using the continuum data sample.
- 3 Tracks misidentified as leptons in $\Upsilon(5S) \rightarrow B_s^{(*)}\bar{B}_s^{(*)}$ events. This background is important for low lepton momentum. It is evaluated using MC simulation of $\Upsilon(5S) \rightarrow B_s^{(*)}\bar{B}_s^{(*)}$ events.
- 4 Residual electrons from photon conversions, muons from charged kaon decays, and leptons from J/ψ decays in $\Upsilon(5S) \rightarrow B_s^{(*)}\bar{B}_s^{(*)}$ events. This background is expected to be small and is also evaluated using $\Upsilon(5S) \rightarrow B_s^{(*)}\bar{B}_s^{(*)}$ MC simulation.

The lepton momentum distribution obtained at the $\Upsilon(4S)$ was corrected to take into account the B meson momentum difference between the $\Upsilon(5S)$ and $\Upsilon(4S)$ samples; this resulted in a smearing (up to $\sim 300 \text{ MeV}/c$ at high lepton momenta) with only a small global effect. To subtract the continuum contribution, lepton momenta are scaled from continuum to the $\Upsilon(5S)$ energy using the same scale factor as for the $x(D_s^+)$ distributions.

The raw lepton momentum distributions for the $\Upsilon(5S)$ sample are shown in Fig. 2, together with the backgrounds discussed above. The background contributions are not large in the momentum region greater than 1.2 GeV/c and are subtracted from the raw $\Upsilon(5S)$ lepton momentum distribution. A small correction is also applied to the electron distribution to take into account the radiative energy losses. Uncertainties in this correction are small and are included in the systematic error. After the background subtraction and the radiative losses correction, the final lepton momentum distributions are corrected for efficiencies. These efficiencies are obtained from MC simulation.

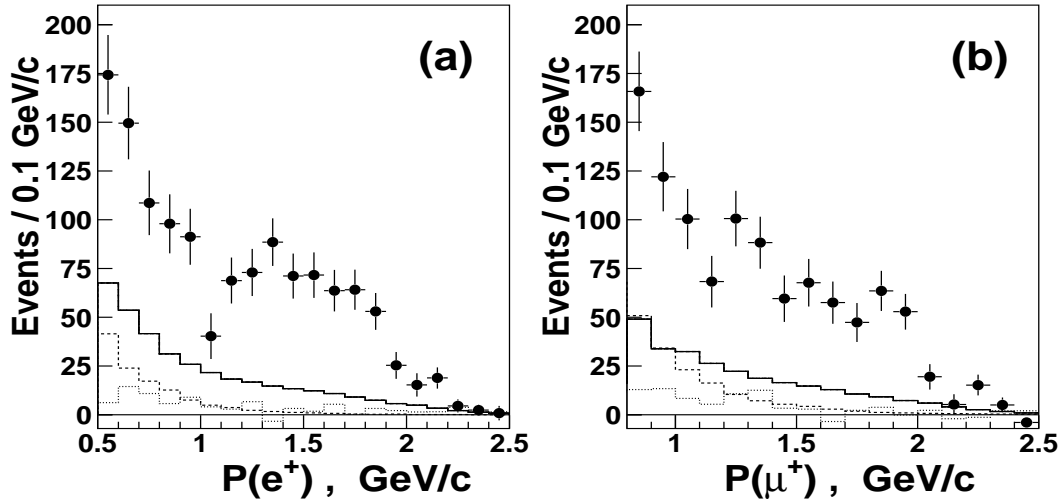


FIG. 2: Raw momentum distributions of electrons (a) and muons (b) in the $\Upsilon(5S)$ sample (data points with error bars), together with estimates of the contributions from background (1) (solid histograms), background (2) (dotted histograms) and backgrounds (3) and (4) (dashed histograms).

SEPARATION OF PRIMARY AND SECONDARY LEPTONS FROM B_s^0 DECAYS

The final lepton momentum distributions, after the background subtraction and efficiency correction, are fitted with the sum of two contributions: one from primary leptons and one from secondary leptons. Primary leptons, produced directly in semileptonic B_s^0 decays, have a momentum spectrum significantly harder than that of secondary leptons, which are produced in the subsequent decays of B_s^0 daughters such as D_s^+ , D^0 and D^+ mesons, and τ^+ leptons. We expect a (5 – 15)% contribution from each of the latter three daughters relative to the D_s^+ contribution. We take the D_s^+ , D^0 , D^+ and τ^+ production ratios from our signal MC simulation to obtain the shape of the secondary lepton momentum distribution, and we vary these ratios within reasonable limits. The resulting systematic uncertainty is found to be small, because the lepton spectra resulting from D_s^+ , D^0 , D^+ and τ^+ decays are similar.

In the fit, we use fixed polynomial parametrizations for both the primary and the secondary lepton momentum spectra as determined from our MC simulation (Fig. 3), which contains the most up-to-date knowledge of specific B_s^0 decays based on experimental measurements and theoretical models. Thus these shapes result from a semi-empirical description of B_s^0 decays.

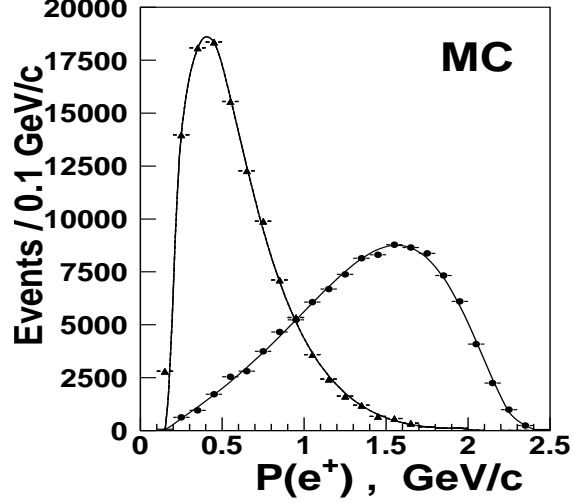


FIG. 3: Momentum distributions of primary (circles) and secondary (triangles) electrons from B_s^0 decays in the MC simulation, superimposed with the polynomial parametrizations used in the final fit (curves).

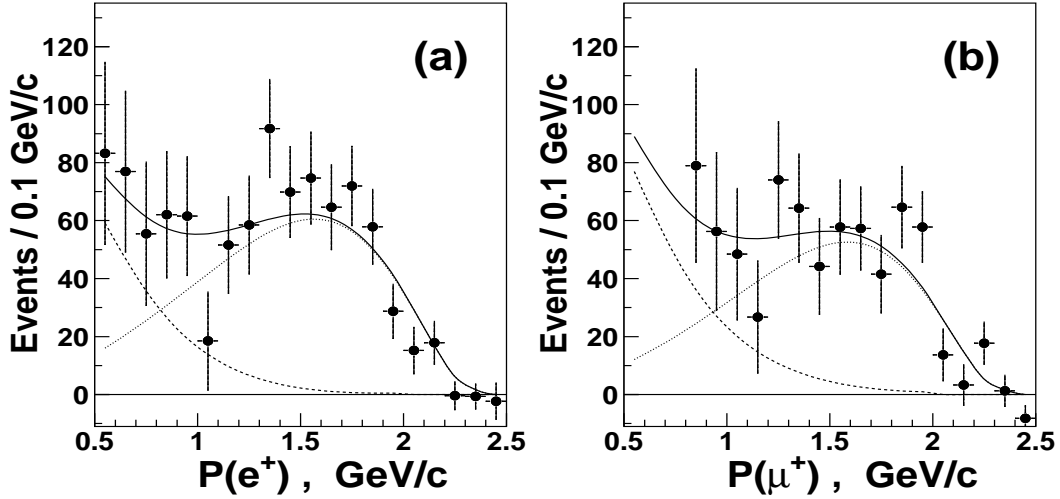


FIG. 4: The electron (a) and muon (b) momentum distributions from B_s^0 decays. The solid curves show the results of the fits, and the dotted curves show the fitted contributions from primary and secondary leptons.

The final leptonic momentum distributions produced in B_s^0 decays (Fig. 4) obtained after background subtractions and an efficiency correction (all corrections described above are also applied) are used to extract the numbers of primary and secondary leptons. We fit the data with a function which includes the sum of two terms with fixed shapes and floating normalizations. Based on the MC simulation, we expect that the momentum ranges selected in our analysis will contain 96.7% of the primary electrons ($P(e^+) > 0.5 \text{ GeV/c}$) and 89.4%

of the primary muons ($P(\mu^+) > 0.8 \text{ GeV}/c$). The only free parameters in the fit are the numbers of primary and secondary leptons. We fit separately the electron spectrum and the muon spectrum, as shown in Fig. 4. We also fit the two distributions simultaneously, assuming equal electron and muon production rates in B_s^0 decays, for both primary and secondary leptons. The results of the three binned χ^2 -fits are given in Table 1. They represent our measured numbers of a same-sign leptons accompanying D_s meson in events with B_s^0 pairs from the $\Upsilon(5S)$ sample.

TABLE I: Results of the electron, muon and combined momentum spectra fits. Numbers of leptons extracted from the fits correspond to the whole momentum region.

Subsample	Number of primary leptons	Number of secondary leptons	Fit, $\chi^2/n.d.f.$
Electron	731 ± 63	430 ± 132	0.99
Muon	619 ± 75	583 ± 334	1.42
Combined	683 ± 46	460 ± 123	1.16

Finally, dividing these numbers by the full number of D_s^+ mesons from B_s^0 decays in our $\Upsilon(5S)$ data sample (see Section 3) and applying an additional factor of 2 due to the B_s^0 mixing effect, we obtain the following semileptonic branching fractions:

$$\mathcal{B}(B_s^0 \rightarrow X^+ e^- \nu) = (10.9 \pm 1.0 \pm 0.9)\% \quad (2)$$

$$\mathcal{B}(B_s^0 \rightarrow X^+ \mu^- \nu) = (9.2 \pm 1.0 \pm 0.8)\% \quad (3)$$

$$\mathcal{B}(B_s^0 \rightarrow X^+ \ell^- \nu) = (10.2 \pm 0.8 \pm 0.9)\%, \quad (4)$$

where the last one represents an average over electrons and muons.

Table 2 lists the systematic uncertainties, which are combined in quadrature to obtain the total systematic uncertainty. Uncertainties due to continuum and $B\bar{B}$ background subtraction are estimated by varying the measured normalization factors by 1.5σ ; the shapes of the distributions are not varied. Uncertainties due to the shapes of the primary and secondary lepton momentum spectra are evaluated by varying them within the expected uncertainties in the B_s^0 decay branching fractions.

The obtained branching fractions can be compared with the PDG value $\mathcal{B}(B^0 \rightarrow X^+ \ell^- \nu) = (10.33 \pm 0.28)\%$, which is theoretically expected to be approximately the same, neglecting a small possible lifetime difference and small corrections due to electromagnetic and light quark mass difference effects.

CONCLUSIONS

The total inclusive semileptonic $B_s^0 \rightarrow X^+ \ell^- \nu$ decay branching fraction is measured for the first time using a 23.6 fb^{-1} data sample collected at the $\Upsilon(5S)$ resonance with the Belle detector at the KEKB asymmetric energy e^+e^- collider. The obtained value, $\mathcal{B}(B_s^0 \rightarrow X^+ \ell^- \nu) = (10.2 \pm 0.8 \pm 0.9)\%$, is in a good agreement with the total inclusive semileptonic B^0 decay branching fraction.

TABLE II: List of systematic uncertainties on the $B_s^0 \rightarrow X^+ \ell^- \nu$ branching fraction measurements.

Source	Relative uncertainty
1. Lepton misidentification	1%
2. Signal and background shapes in D_s^+ mass fit	3%
3. Determination of full D_s^+ meson number	4%
4. Continuum background modeling	2%
5. $B\bar{B}$ background modeling	2%
6. MC lepton efficiency determination	4%
7. Variation of D^0 , D^+ and τ^+ contributions	1%
8. Shapes of primary and secondary lepton momentum spectra	5%
Sum in quadrature	8.5%

ACKNOWLEDGMENTS

We thank the KEKB group for the excellent operation of the accelerator, the KEK cryogenics group for the efficient operation of the solenoid, and the KEK computer group and the National Institute of Informatics for valuable computing and Super-SINET network support. We acknowledge support from the Ministry of Education, Culture, Sports, Science, and Technology of Japan and the Japan Society for the Promotion of Science; the Australian Research Council and the Australian Department of Education, Science and Training; the National Science Foundation of China and the Knowledge Innovation Program of the Chinese Academy of Sciences under contract No. 10575109 and IHEP-U-503; the Department of Science and Technology of India; the BK21 program of the Ministry of Education of Korea, the CHER SRC program and Basic Research program (grant No. R01-2005-000-10089-0) of the Korea Science and Engineering Foundation, and the Pure Basic Research Group program of the Korea Research Foundation; the Polish State Committee for Scientific Research; the Ministry of Education and Science of the Russian Federation and the Russian Federal Agency for Atomic Energy; the Slovenian Research Agency; the Swiss National Science Foundation; the National Science Council and the Ministry of Education of Taiwan; and the U.S. Department of Energy.

-
- [1] W.-M. Yao *et al.* (Particle Data Group), J. Phys. G **33**, 1 (2006).
 - [2] M. Artuso *et al.* (CLEO Collaboration), Phys. Rev. Lett. **95**, 261801 (2005).
 - [3] G. Bonvicini *et al.* (CLEO Collaboration), Phys. Rev. Lett. **96**, 022002 (2006).
 - [4] A. Drutskoy *et al.* (Belle Collaboration), Phys. Rev. Lett. **98**, 052001 (2007).
 - [5] A. Drutskoy *et al.* (Belle Collaboration), Phys. Rev. D **76**, 012002 (2007).
 - [6] I. Bigi, B. Blok, M. A. Shifman and A. Vainshtein, Phys. Lett. B **323**, 408 (1994).
 - [7] A. F. Falk, M. B. Wise and I. Dunietz, Phys. Rev. D **51**, 1183 (1995).
 - [8] E. Bagan, P. Ball, V. M. Braun and P. Gosdzinsky, Phys. Lett. B **342**, 362 (1995).
 - [9] M. B. Voloshin, Phys. Rev. D **51**, 3948 (1995).

- [10] M. Neubert and C. T. Sachrajda, Nucl. Phys. B **483**, 339 (1997).
- [11] S. Kurokawa and E. Kikutani, Nucl. Instr. and Meth. A **499**, 1 (2003) and other papers included in this Volume.
- [12] A. Abashian *et al.* (Belle Collaboration), Nucl. Instr. and Meth. A **479**, 117 (2002).
- [13] K. Hanagaki *et al.*, Nucl. Instr. and Meth. A **485**, 490 (2002).
- [14] A. Abashian *et al.*, Nucl. Instr. and Meth. A **491**, 69 (2002).